Thin Solid Films 519 (2011) 3538–3543

Contents lists available at ScienceDirect

Thin Solid Films

journal homepage: www.elsevier.com/locate/tsf

Effect of samarium addition and annealing on the properties of electrodeposited ceria thin films

L. Živković [a,b], V. Lair [a,*], O. Lupan [a,c], A. Ringuedé [a]

[a] Laboratoire d'Electrochimie, Chimie des Interfaces et Modélisation pour l'Énergie, LECIME, CNRS UMR 7575, Chimie ParisTech (ENSCP)-Paris, 11 rue Pierre et Marie Curie, 75231 Paris cedex 05, France
[b] The Vinča Institute of Nuclear Sciences, University of Belgrade, 11 001 Belgrade, PO BOX 522, Serbia
[c] Department of Microelectronics and Semiconductor Devices, Technical University of Moldova, 168 Stefan cel Mare Blvd., Chisinau, MD-2004, Republic of Moldova

ARTICLE INFO

Article history:
Received 4 February 2010
Received in revised form 5 January 2011
Accepted 12 January 2011
Available online 27 January 2011

Keywords:
Samarium-doped ceria
Electrodeposition
Thin films
Fuel cells
X-ray diffraction
Raman spectroscopy

ABSTRACT

Samarium (Sm)-doped ceria (CeO_2) (SDC) is a promising material for high temperature electrochemical devices. Our work demonstrates that thin SDC films can be prepared by a cost-effective electrodeposition method at a low-temperature (30 °C) and −0.8 V/SCE (saturated calomel electrode) potential. Analysis of the structural properties of the obtained SDC films, as-grown and annealed at 600 °C, has been carried out by X-ray diffraction (XRD). Morphology and film composition were studied using scanning electronic microscopy and energy dispersive X-ray analysis. Vibrational properties were determined by Raman spectroscopy. The effects of samarium addition into the deposition bath on the final film composition have been studied. According to XRD results, film crystallographic properties are directly linked to the percentage of Sm incorporated in the CeO_2 lattice. We report on the electrochemical deposition of the SDC films performed over a large range of Sm additions (0–30%). The effect of temperature annealing has been studied as well.

© 2011 Elsevier B.V. All rights reserved.

1. Introduction

Cerium oxide or ceria (CeO_2) is a rare earth oxide that has attracted much attention for the variety of technological applications due to its ability to store, release or transport oxygen. Pure and doped-ceria are widely used in many different catalytic fields, such as oxygen sensors [1,2] or powerful hydrocarbon oxidation catalysts [3,4]. One of the most promising applications for ceria layers is in Solid Oxide Fuel Cells (SOFC). They can be used as an interfacial catalytic layer, a chemical diffusion barrier, or as an electrolyte material when doped [5–7]. SOFCs are high-energy conversion systems and low-pollution devices, but the operating temperature is still high (about 1000 °C) and depends on the solid electrolyte used. It is known that pure CeO_2 is a poor oxide ion conductor [8]. However, ionic conductivity can be improved by an appropriate doping at a lower temperature (below 800 °C) [9]. It was reported that its conductivity can be remarkably enhanced by increasing the concentration of oxygen vacancies after doping with Sm, due to Ce^{4+} substitution and formation of oxygen vacancies, following this reaction [8]: $Sm_2O_3 \xrightarrow{CeO_2} 2Sm'_{Ce} + 3O_O^{\times} + V_O^{\cdot\cdot}$. In this context, samarium (Sm)-doped ceria (SDC) was reported to exhibit the highest ionic conductivity at fixed doping levels among the rare-earth-doped ceria, as the radius of the dopant ion is close to that of the host cation [10,11]. Due to the possibility of mixed ionic and electronic conductivity, mainly under a reducing atmosphere such as hydrogen, SDC is also used as an anode material. Thus, SDC was shown to improve electrode performance, enhancing its electrochemical activity when used as an integral component in the anode cermet or as a thin functional interlayer between electrode and electrolyte [12–14]. In addition, doped ceria can find applications in Molten Carbonate Fuel Cell. Along with the above mentioned applications in electrochemical devices, the ceria-based coating could be beneficial against corrosion of stainless steel bipolar plates that serve as interconnects [15,16].

A variety of physical and wet-chemical methods are available in the literature for the synthesis of the SDC material, such as electron beam deposition [17], microwave induced combustion [18], sol–gel [19], spray pyrolysis [20], homogeneous precipitation [21], and hydrothermal synthesis [22]. However, electrodeposition has attracted great interest as a powerful low-cost technique for the processing of high quality films on any shaped substrates, at room temperature and ambient pressure and can be easily scaled up for industrial applications. As widely discussed in the thin film literature, the electrodeposition process of ceria is based on the local interfacial pH change in the vicinity of the electrode by means of cathodic reduction of the oxygen precursor [23–28]. In previous papers, a detailed study on the synthesis and characterization of undoped ceria was reported [29,30]. Recently, Ruiz et al. [31] demonstrated that the formation mechanism of samarium coatings was similar to the ceria one. However, studies on the electrodeposition method for producing

* Corresponding author.
E-mail address: virginie-lair@ens.chimie-paristech.fr (V. Lair).

0040-6090/$ – see front matter © 2011 Elsevier B.V. All rights reserved.
doi:10.1016/j.tsf.2011.01.245

samarium-doped ceria films are still quite limited [32–34]. In this paper we highlighted the possibility to tune the physical and chemical properties of ceria by a doping process. The effect of annealing on SDC properties, was emphasized as an important step [35].

The current work presents our research towards the electrochemical preparation of samarium-doped ceria thin films. Electrodeposition via a potentiostatic mode was used for the preparation of films, at 30 °C. We first report on the electrochemical deposition of the SDC films performed under a large range of Sm concentrations. Detailed analyses of the structural, morphological and vibrational characteristics of SDC films are then presented. The effects of thermal annealing on the SDC properties are given as well, in view of compatibility and stability in conditions closer to SOFC working ones.

2. Experimental details

The deposition solutions, containing 0.05 M $Ce(NO_3)_3.6H_20$ (Alfa Aesar, 99.5%) and 0.1 M $NaNO_3$ (Riedel de Haen, 99.5%) were prepared with deionized water (electrical resistivity 18.2 MΩ cm). A series of Sm $(NO_3)_3.6H_20$ (Alfa Aesar, 99.9%) additions were performed, in the range 0–30%, calculated on the base of cerium nitrate molar concentration. The solutions were saturated with molecular oxygen for 1 h before starting the experiment, and a slight O_2 bubbling in the reactor bath was maintained during the deposition process. The electrodeposition was performed in a classical three electrode experimental set-up, with a 316L stainless steel sample as working electrode ((Goodfellow), diameter 0.7 cm), a platinum wire as counter-electrode and a saturated calomel electrode (SCE) as reference (E = + 0.24 V/ENH). The substrate (stainless steel) was abraded using SiC 800 paper, then cleaned in ethanol for 5 min under ultrasonics, rinsed with deionized water, and dried with a pulsed air flux immediately before the deposition. The substrate was fixed to the rotating electrode (300 rpm). The bath temperature was fixed at 30 °C. Films were obtained by a potentiostatic method, applying a −0.8 V/SCE potential, using an EG&G Instruments, model 263A, Princeton Applied Research. Electrodeposition was performed for 2 h. After the deposition, samples were rinsed in deionized water and dried under ambient conditions. In order to study the effect of thermal treatment on the SDC films, one set of as-grown samples was annealed at 600 °C for 1 h, with a slow heating rate of 2 °C per minute. X-ray diffraction (XRD) was performed using a Siemens D5000 instrument (with 40 kV and 45 mA generator settings; scan type was continuous, step size 0.03° (2θ) between 10 and 100°). The crystallite size (D) was determined from the broadening of the (111) diffraction peak, taking into account the instrumental broadening. The X'pert Database 32 software with the integrated Scherrer formula [36] was used ($D = 0.90\lambda/\beta_{1/2}\cos\theta$, where λ is the wavelength for $Cu_{K\alpha1}$ (0.15405 nm) radiation and $\beta_{1/2}$ is the width at half-height of the diffraction profile).

SEM (scanning electron microscopy) images were recorded using a high resolution Ultra 55 Zeiss FEG scanning electron microscope with an acceleration voltage of 10 kV. Energy dispersive X-ray spectroscopy (EDX) analyses were performed with a Bruker Li-drift silicon detector.

Micro-Raman spectra were measured at room temperature with a Horiba Jobin system (HR800 UV) in a backscattering configuration. A 632.8 nm line of a He–Ne laser was used for off-resonance excitation. The instrument was calibrated to the same accuracy using a naphtalene standard.

3. Results and discussion

Electrodeposition of a series of samples from the deposition baths containing 0–30% Sm (III) at fixed Ce (III) concentration (0.05 M) was performed. Table 1 summarizes the compositions used in the experiments.

Table 1
Composition of electrolytic baths, prepared at Ce (III) (0.05 M) with different Sm (III) amounts added (denoted both in mol % and in mM) used for growing SDC samples.

Sm (III), mol %	0	0.4	0.6	1	1.5	2	5	10	15	30
Sm (III), mM	0	0.2	0.3	0.5	0.75	1	2.5	5	7.5	15

The obtained SDC films, as-grown and annealed, were analyzed in detail regarding their various properties as presented further in the study.

3.1. Structural characterization

Fig. 1 illustrates X-ray diffraction patterns of as-deposited SDC films, obtained with different concentrations of Sm (III) in the solution bath (up to 2%), according to Table 1. All patterns display diffraction peaks corresponding to (111), (200), (220) and (311) planes, which match well with the cubic fluorite CeO_2 crystal structure, referring to JCPDS# 34-0394 standard data. From the more intense peak, (111), crystallite sizes have been calculated. An increase of the Sm content, even in a small amount, induces an enhancement of the CeO_2-based phase crystallinity. Despite the broad diffraction lines, typical of small crystallites [37], it has been evaluated around 5.9, 6.3, 8.7 and 10.2 nm, for 0, 0.4, 0.6 and 1.0% Sm, respectively.

However, with a further increase in the Sm content from 1.0 to 1.5%, the intensity of CeO_2 peaks decreases, and crystallite size drops to 5 nm. At 2% Sm content, (111) and (200) diffraction peaks cannot be observed in XRD patterns. The related X-ray pattern indicates an amorphous structure. The same result was obtained for the samples prepared at the Sm content from 5 to 30%. Based on our experimental data, it can be concluded that a Sm content greater than 1.0% suppresses ceria crystallization. Our result is in accordance with the findings of Phok et al. [32,33] who showed that ceria exhibited lower or better crystallinity, depending on the Sm doping amount. Recently, Kamada et al. [34] presented the XRD spectra of electrodeposited Sm-doped ceria displaying lower crystallinity in comparison with pure ceria. Several authors [35–39] also reported a decrease in the ceria crystallite size with increasing Sm doping. So far, the origin of this phenomenon is still not fully understood.

Fig. 2 shows the XRD pattern of the Sm-doped ceria in the 0–2% range, as well as a 15% Sm film sample, after annealing at 600 °C for 1 h in air. Comparison with as grown films shows a similar tendency regarding the effect of the Sm content on crystallinity. An increase in the (111) peak intensity with Sm doping from 0 to 1% Sm (curves (1) and (2)) is seen, followed by a decrease in crystallinity with higher Sm doping (>1%). However, a broad and weak diffraction line (curve 3, Fig. 2) corresponding to the (111) peak appeared at 2% Sm content,

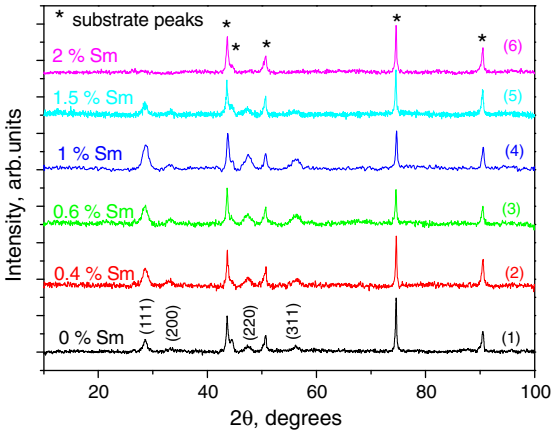

Fig. 1. XRD patterns of electrodeposited Sm-doped ceria films as a function of Sm (III) concentrations added in the deposition bath in the range 0–2% Sm. Normalized intensity versus the stainless steel peak at 2θ = 43.69°.

Download English Version:

https://daneshyari.com/en/article/1668858

Download Persian Version:

https://daneshyari.com/article/1668858

Daneshyari.com